SAND2017-6083PE

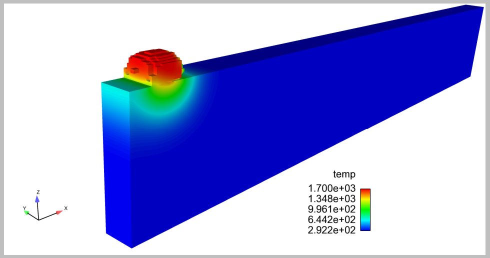

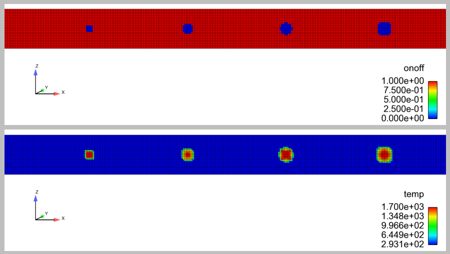

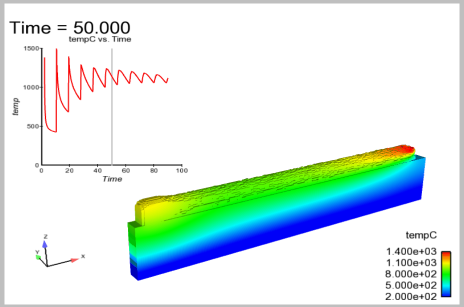

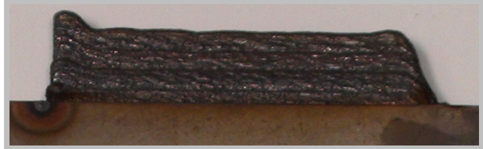

LENS Process Modeling Update – UC Davis Collaboration

C. Alleman M. E. Stender, L. L. Beghini, M. G. Veilleux, S. R. Subia, J. D. Sugar

June 13th, 2017

Sandia National Laboratories is a multimission laboratory managed and operated by National Technology and Engineering Solutions of Sandia, LLC., a wholly owned subsidiary of Honeywell International, Inc., for the U.S. Department of Energy's National Nuclear Security Administration under contract DE-NA0003525.

Lifecycle Analysis of Additively Manufactured Components

Process Design and Simulation

Advanced process controls and diagnostics enable simulation tools to "grow" near-net-shape structure

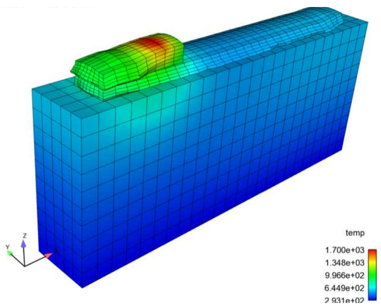

Microstructure and Properties

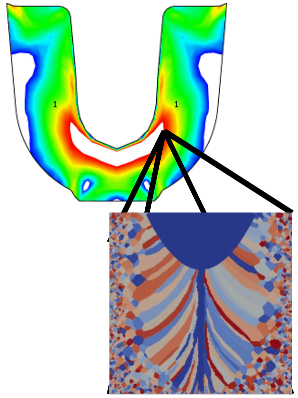

Internal state variable models account for microstructural evolution and distribution of properties (related to spatial variations of thermal history)

Residual Stresses

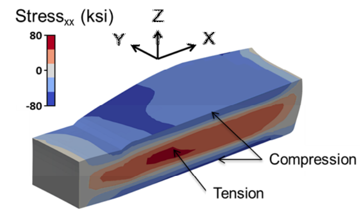

Solidification and thermal history result in strong residual stresses, which can impact performance

- Predictive uncertainties result in large safety factors, reduced lifetimes, and increased costs.
- Our approach develops tools to reduce uncertainty, increase understanding, and enhance predictive capability.

Assembly and Service

Multiphysics approaches for fully coupled simulation of chemical/thermal transport, mechanical loading, etc. to predict performance

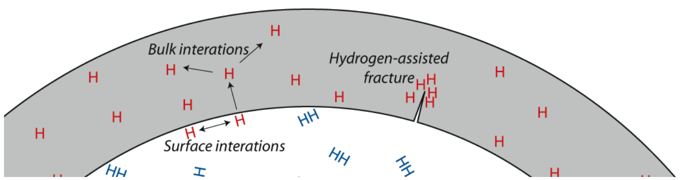

(includes unique service environments, such as hydrogen embrittlement, corrosion, microstructural aging, etc)

Crack Initiation, Growth and Failure

Transition from crack initiation to failure is not well characterized and depends on microstructure and defects

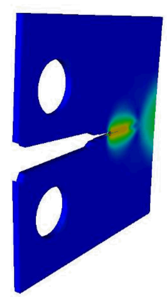

Margin/Uncertainty → Design Life

Service requirements may dictate design iteration to assure sufficient margin based on predictive uncertainties. The lifecycle analysis provides a tool to enable design optimization to meet the requirements.

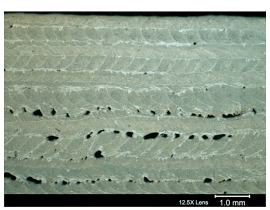

Process Modeling of LENS Manufacturing

Sandia National Laboratories

Step 1 Thermal Activation

Initial mesh:

Deposition Block
- Zero conductivity
- Initially inactive

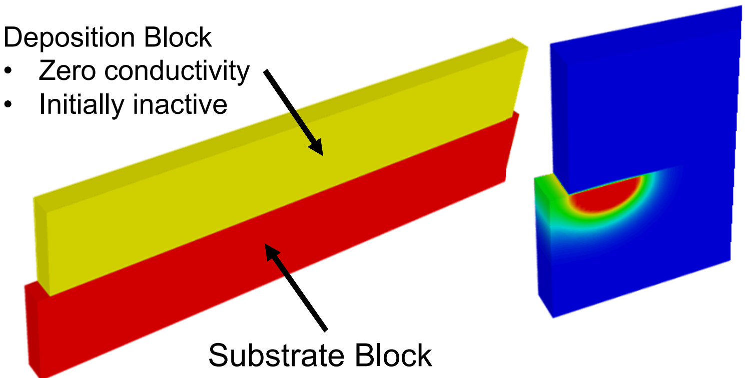

Step 2 Remove Inactive Elements

- Remove elements that are below melt temperature
- Create surfaces for radiation and convection

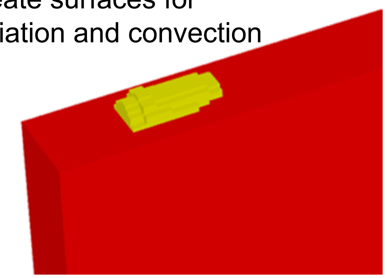

Step 3 Thermal Analysis

- Radiation, convection, and conduction

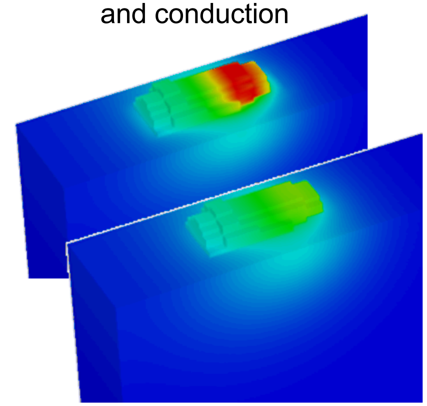

Step 4 Map and/or Initialize Mechanical Variables

- Map material state variables and displacements from previous solid mechanics solution
- Newly activated elements are given initial material parameters

Step 5 Structural Analysis

- Calculate residual stresses as a result of thermal gradients
- Solid elements (below melt temperature)
  - Solid material properties
  - Tied contact
- Fluid elements
  - Newtonian fluid material model
  - Sliding frictional contact

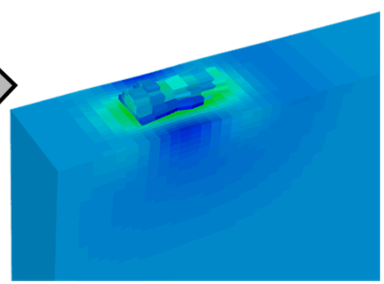

* Displacements shown 15x

Step 6 Map Back to Reference Configuration

- Map material state variables, displacements, and temperatures back to original mesh

Spherical Moving Heat Source

- Material is activated via a spherical, volumetric heat source
  - Inputs: raster path, melt temperature, diameter, efficiency, radius and spatial influence factor
  - Activation user variable – tracks element activation status
  - Zero conductivity in deposition block
    - Laser heat absorbed by specific heat of deposition material within the laser spatial influence
    - Heat not transferred to inactive material

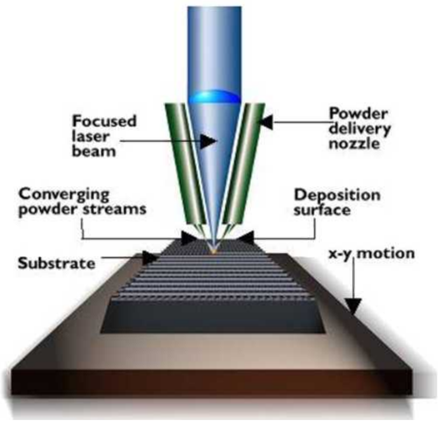

LENS Process

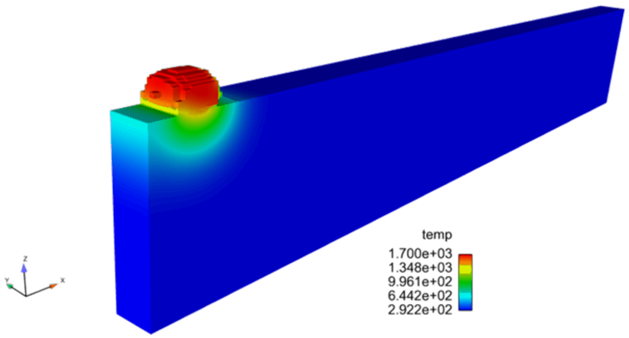

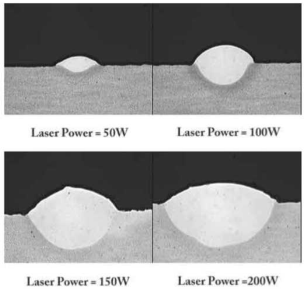

Figure 2: Cross-sectional photographs showing semi-circular type melt pool geometry over a range of laser powers. Travel speed = 5 mm/s, powder mass flow rate = 0.08 g/s.

http://www.lehigh.edu/~inemg/Framset/Research_Activities/JLP/LENS/LENS_4.htm

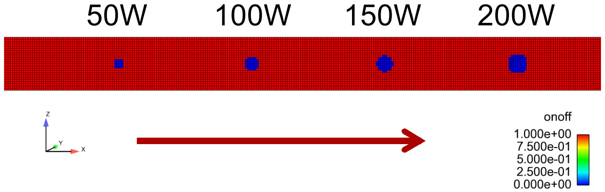

activated elements increases with power

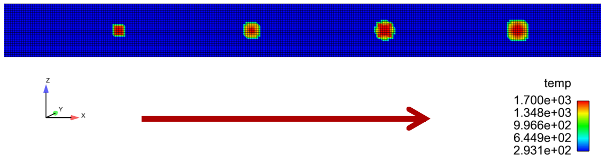

Melt pool size increases with power

LENS Button Modeling

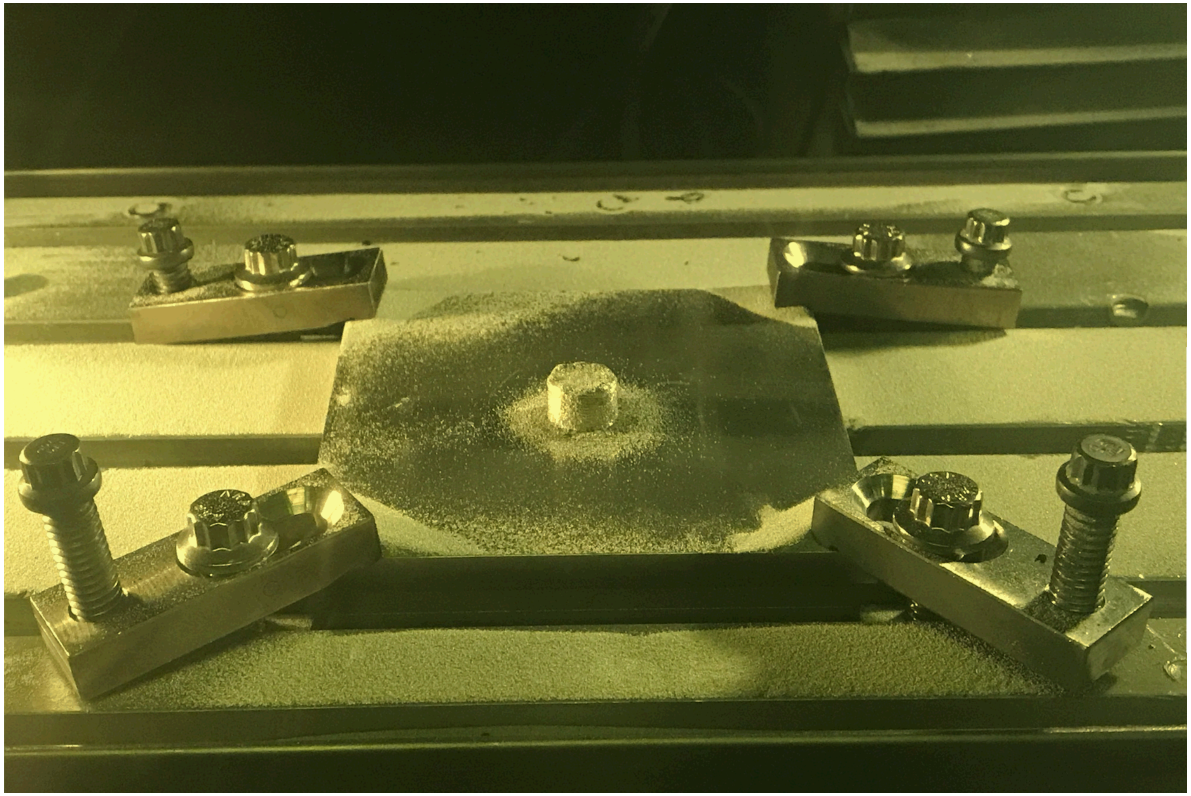

- ½" high
- ½"diameter
- 4"x4"x1/4" plate
- 304 L Stainless Steel

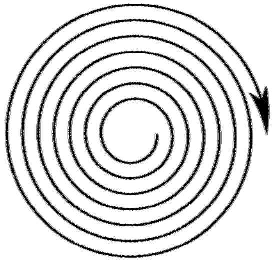

Build Pattern

Modeling Update:

- Explicit model ~½ way through printing
- Implicit models implemented and running ~1/8 way through print
- Contact removed to improve calculation speed
- Exploring sensitivity to activation parameters – laser diameter, power, mesh density, *etc*. to improve calculation turnaround time

New Mechanical Boundary Conditions Implemented in Implicit Model

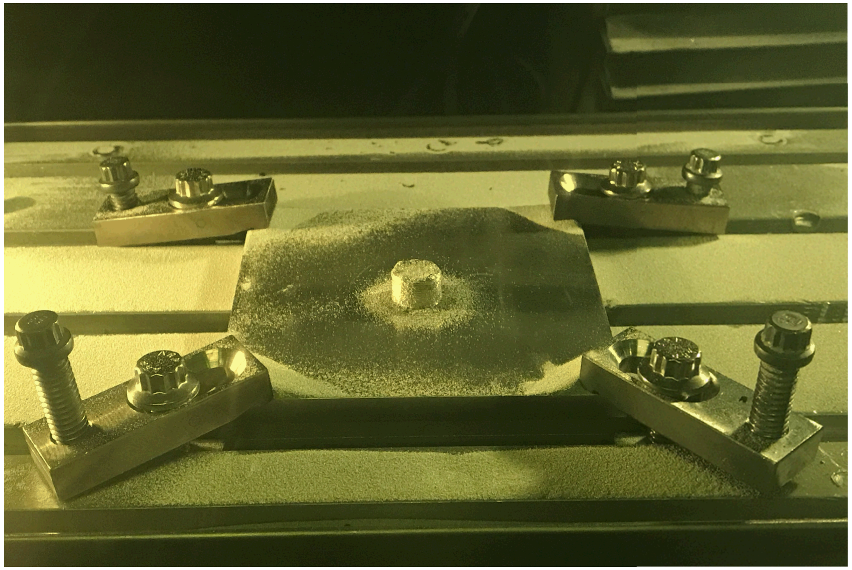

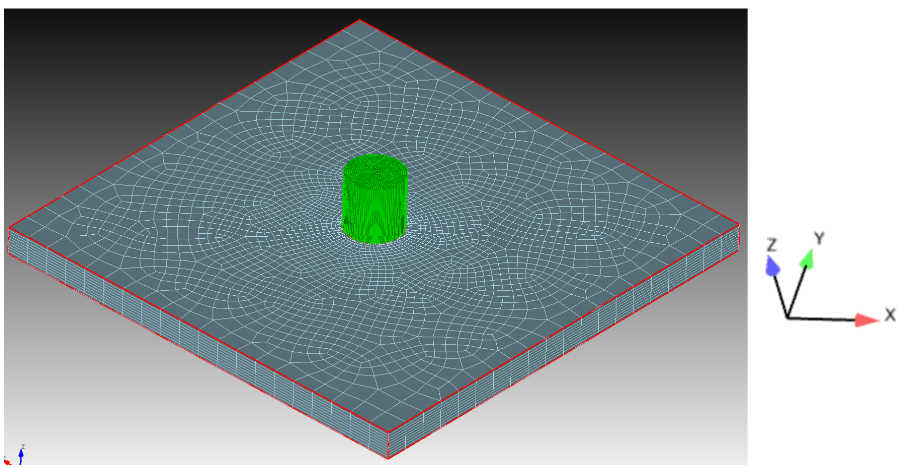

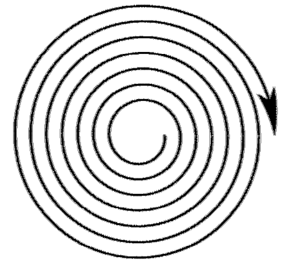

Build Pattern

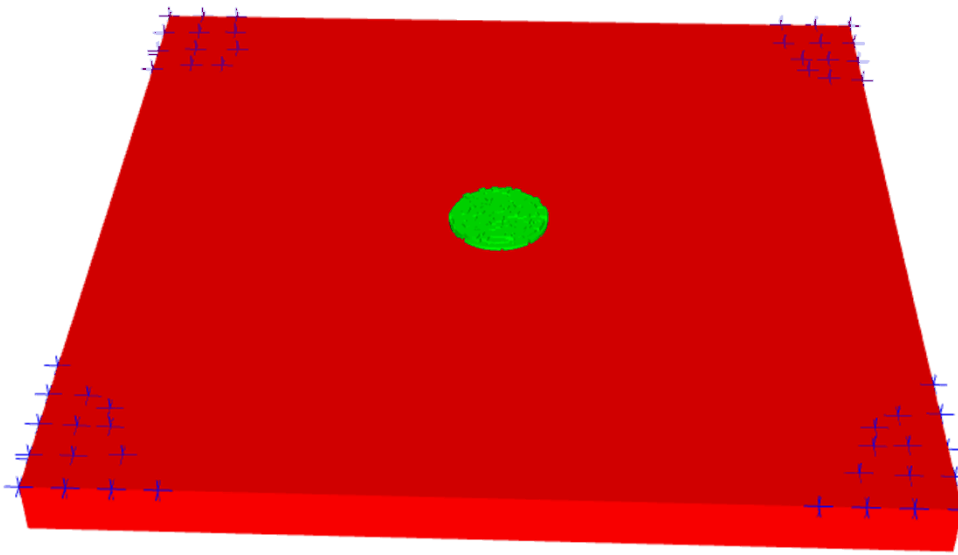

- Blue checks correspond to fixed displacement nodes – reminiscent of clamping
  - Previous models fixed displacements on the bottom of the build plate

Explicit Thermal Mechanical Modeling

- First layer of deposition in explicit model
  - Spiral build pattern to match experimental raster path

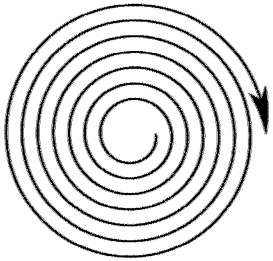

Build Pattern

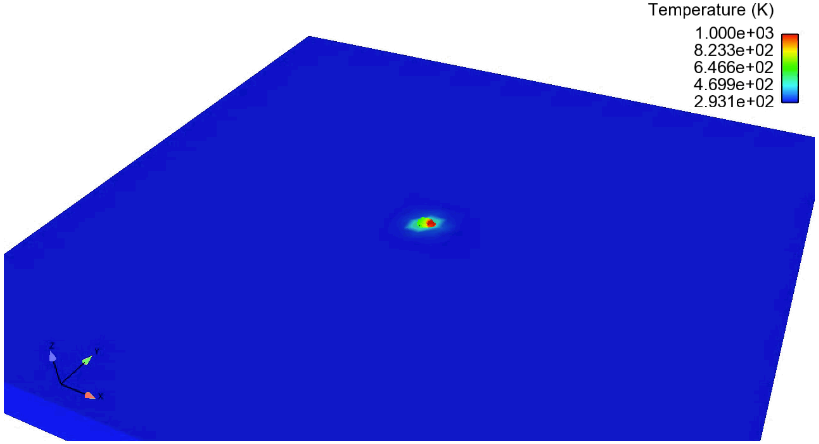

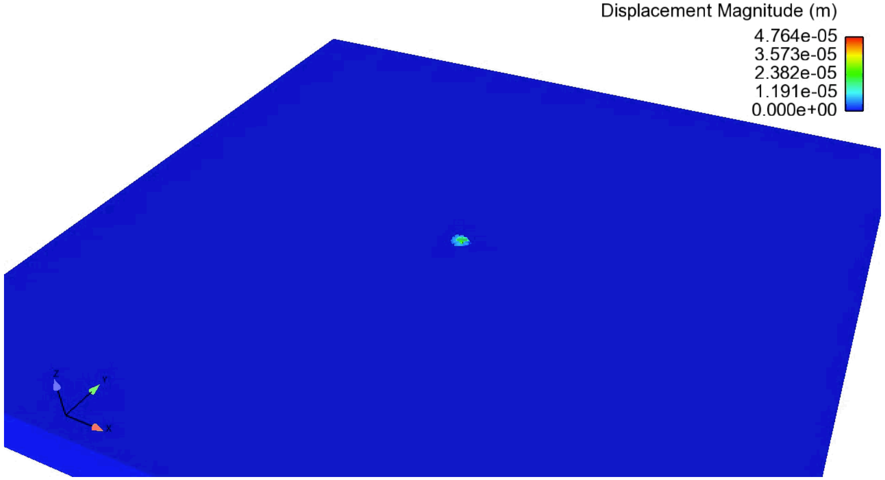

Residual Stresses and Plastic Strains

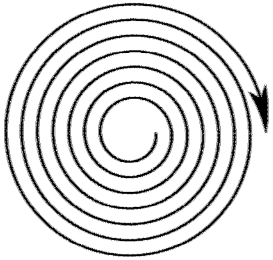

Build Pattern

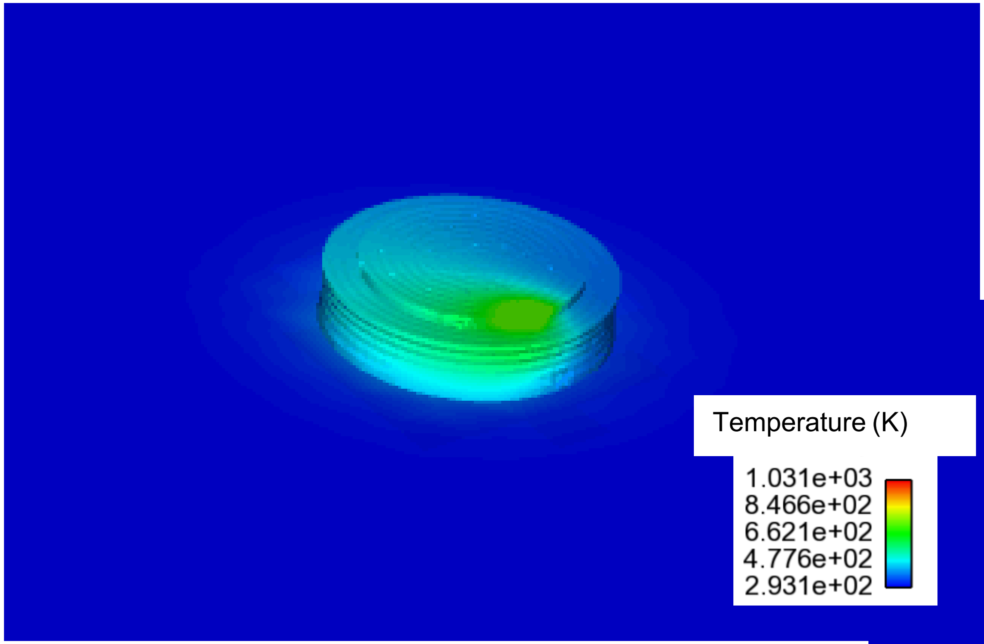

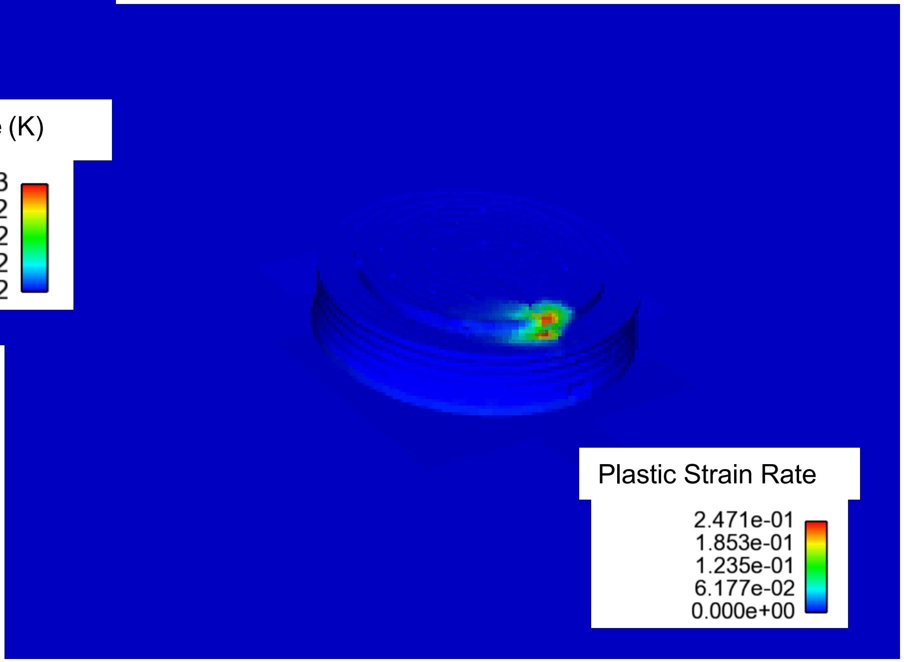

Nonzero plastic strain rate corresponds to high temperature regions

Explicit Simulations at 50% of Complete Build Time

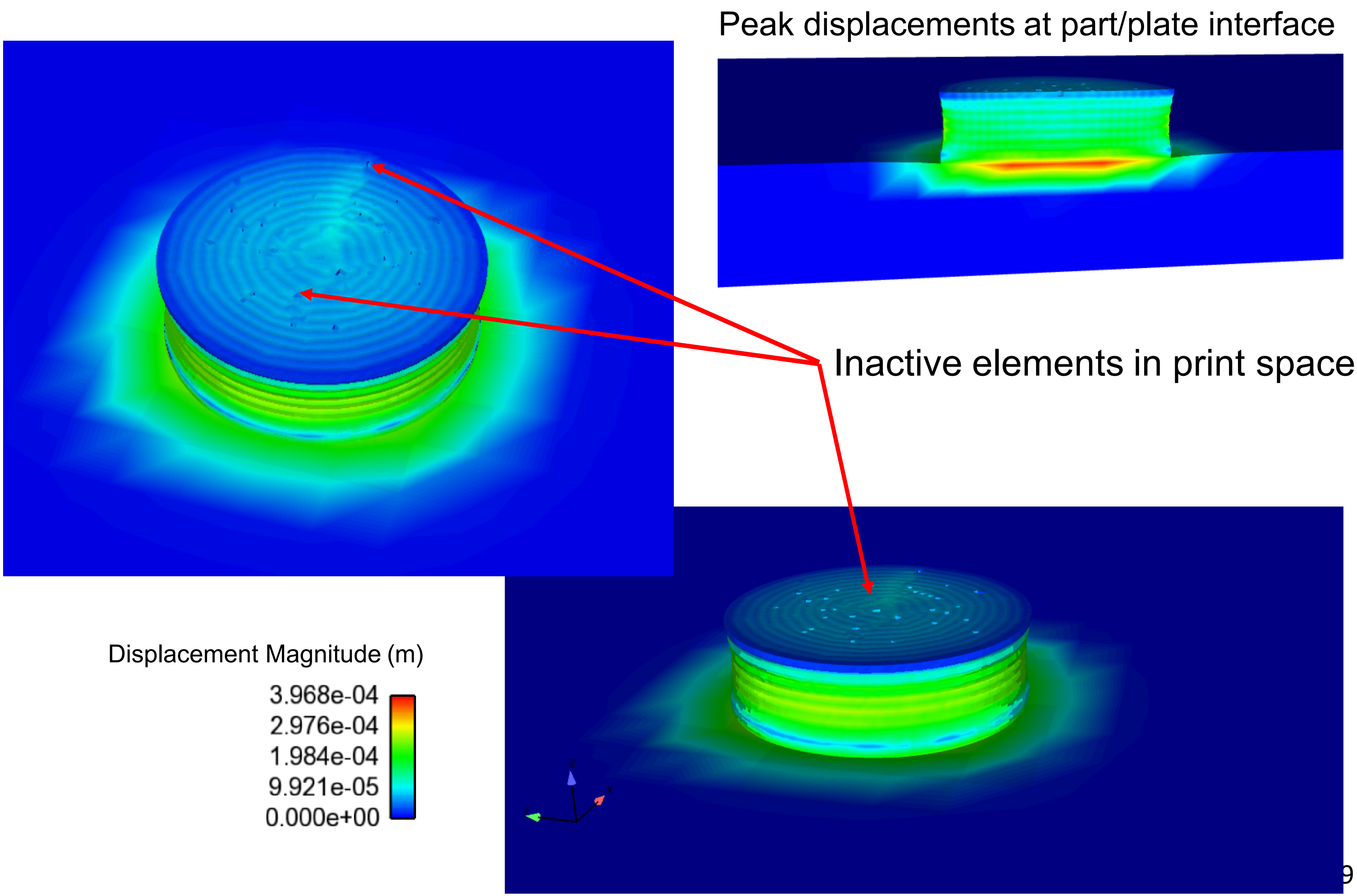

Hardness Values are Higher Near Baseplate

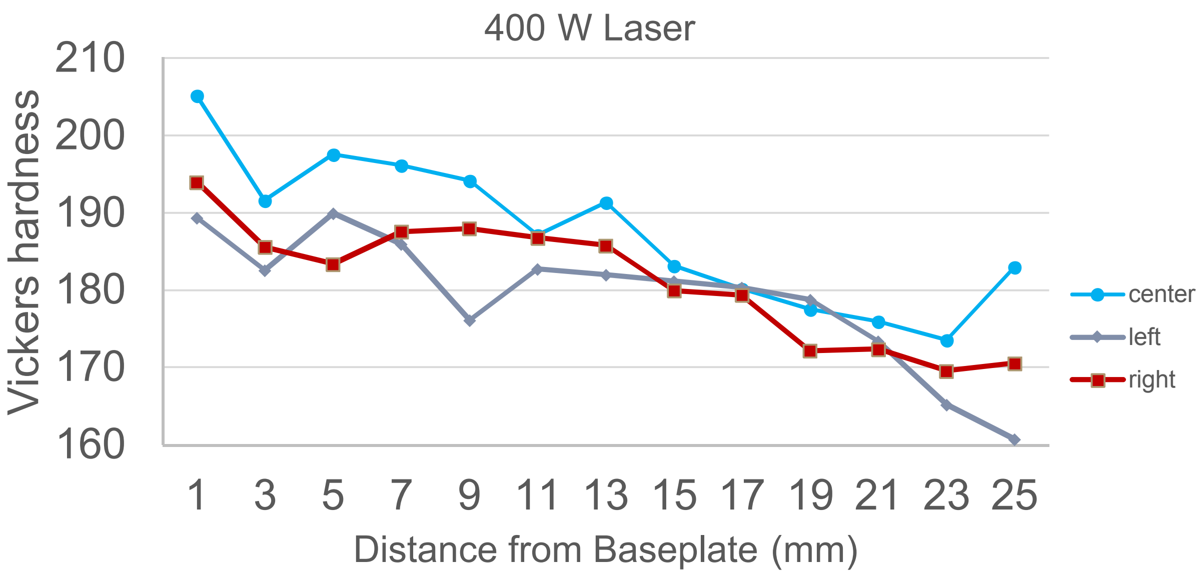

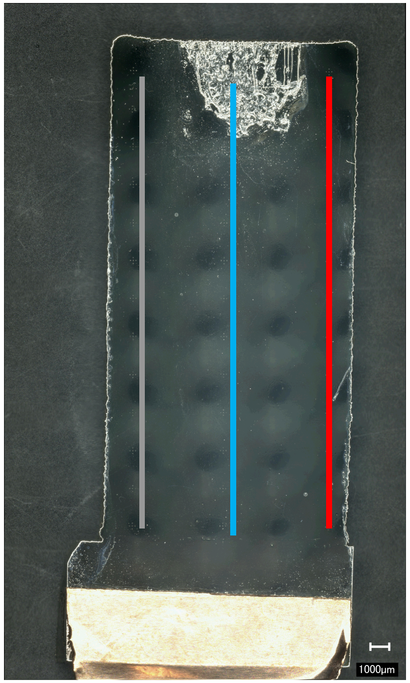

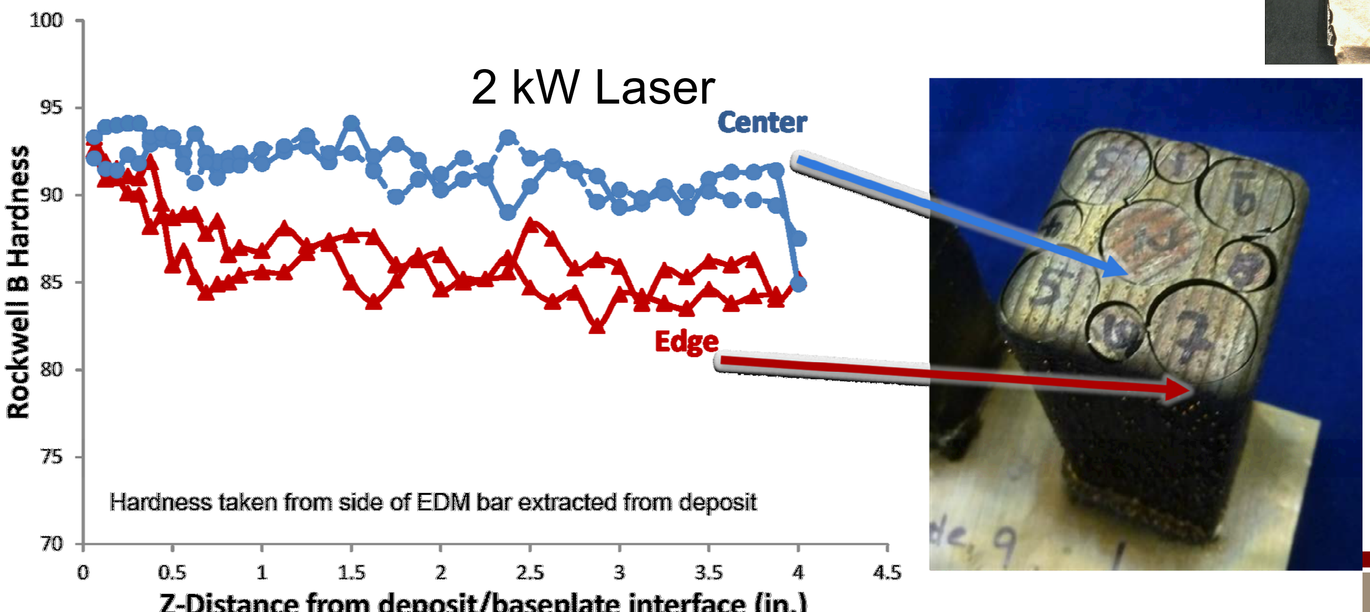

Several Fine-Scale Features to Consider in the Overall Microstructural Picture

Sandia National Laboratories

Finely Distributed Ferrite

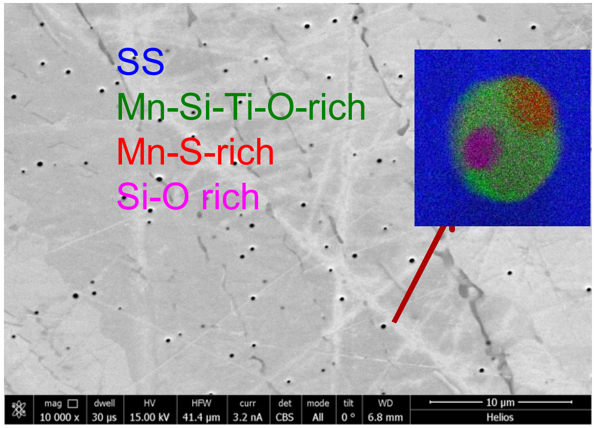

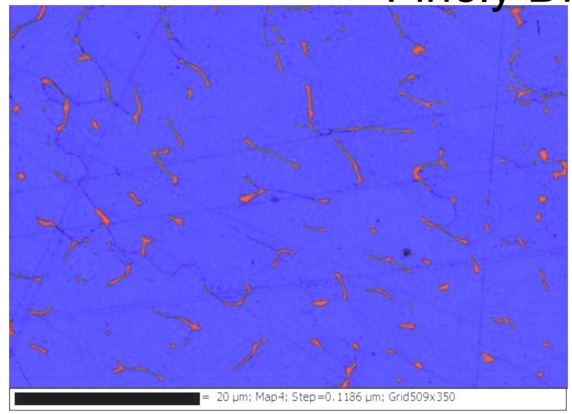

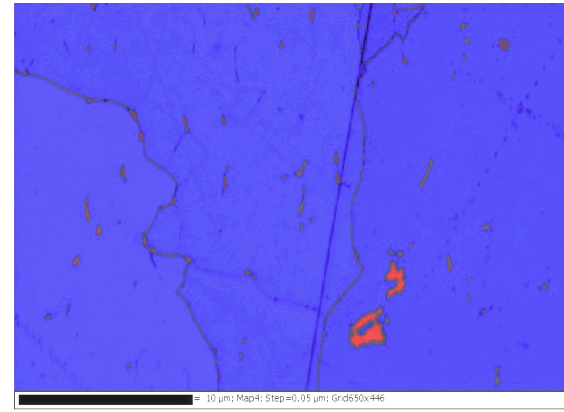

20 µm 2 kW PSU

10 µm 400 W

2 kW P

CD 316

None show an obvious significant variation with distance from baseplate

Oxide Par

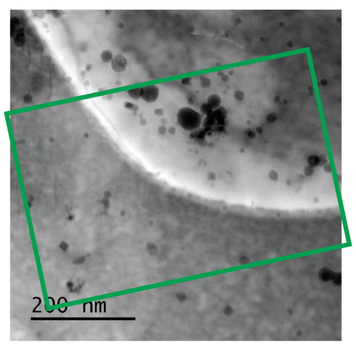

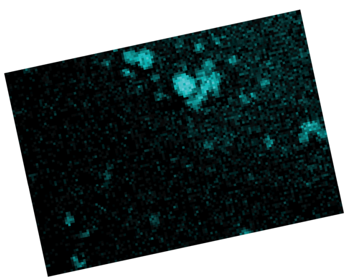

Cr-O rich

400 W UCD 316

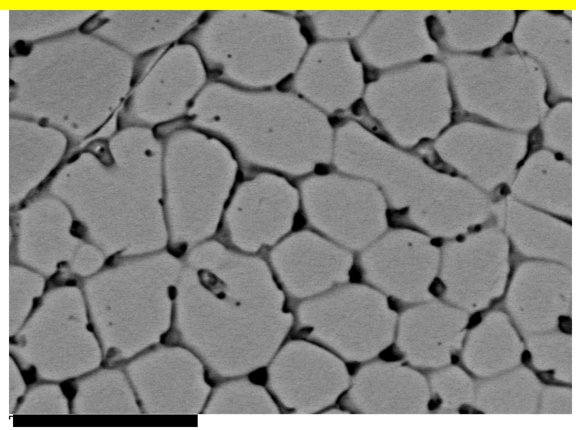

10 µm

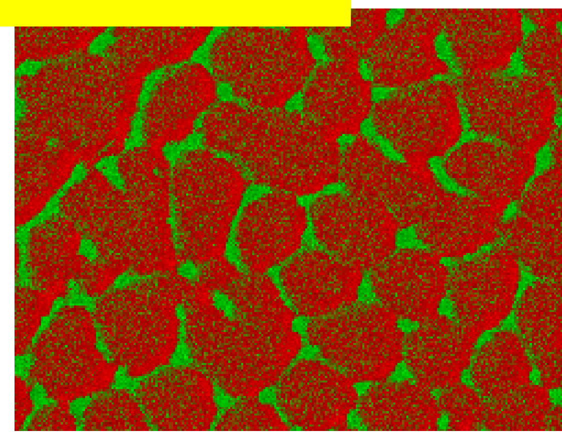

Cellular Solidification Structure

Cr-rich

Ni-rich

Dislocation Structure Depends on Location in Build

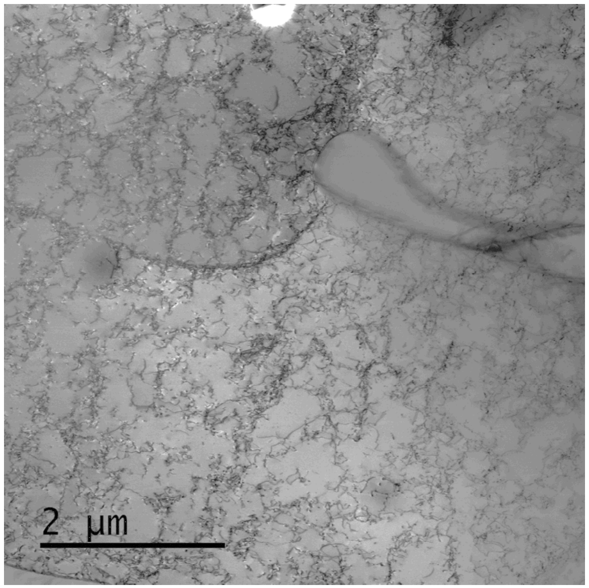

2 mm from Base BF STEM

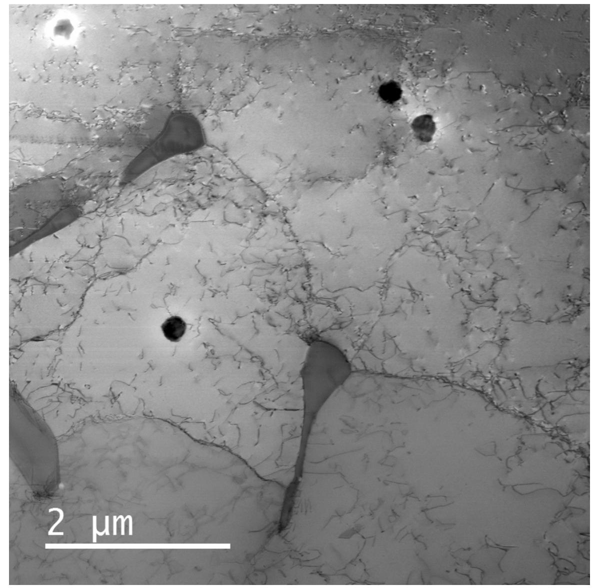

2 mm from Top BF STEM

- Qualitatively, there appear to be less dislocations near the top of the build
- This correlates with lower hardness numbers near the top of the build

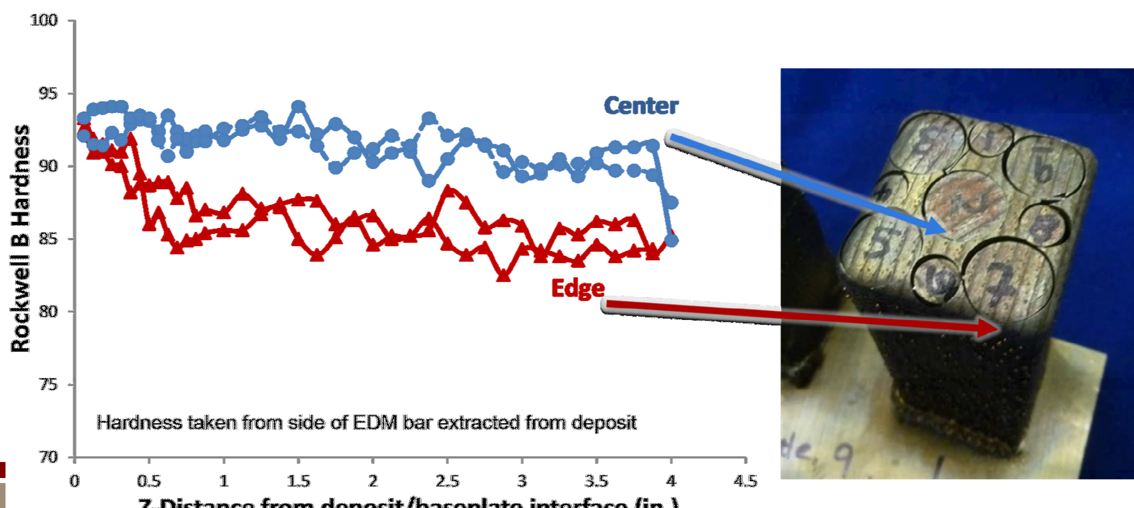

Measurement of Geometrically Necessary Dislocations with EBSD

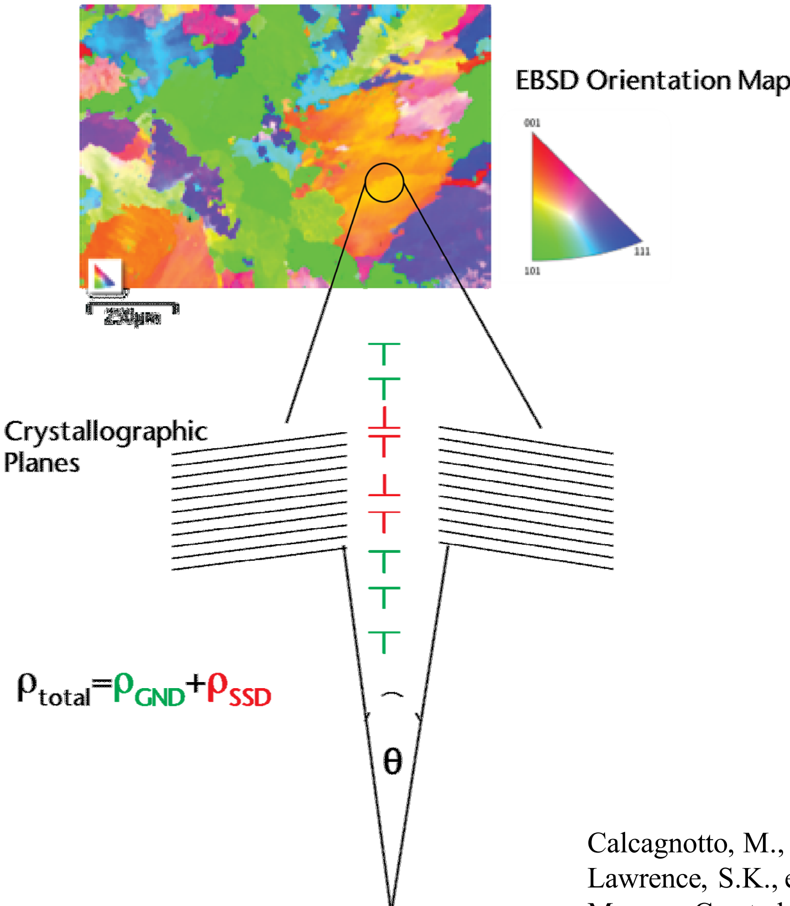

$\rho_{total} = \rho_{GND} + \rho_{SSD}$

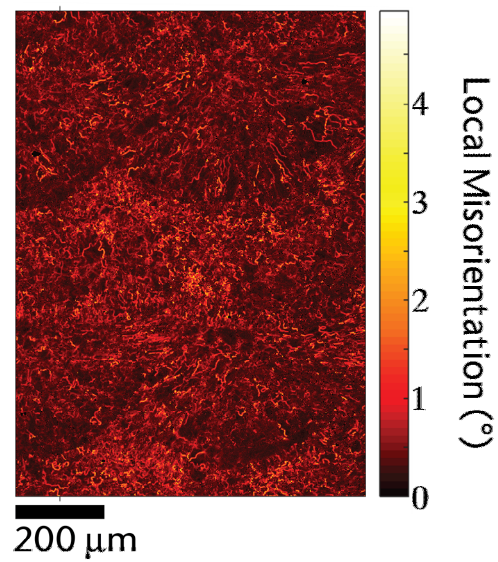

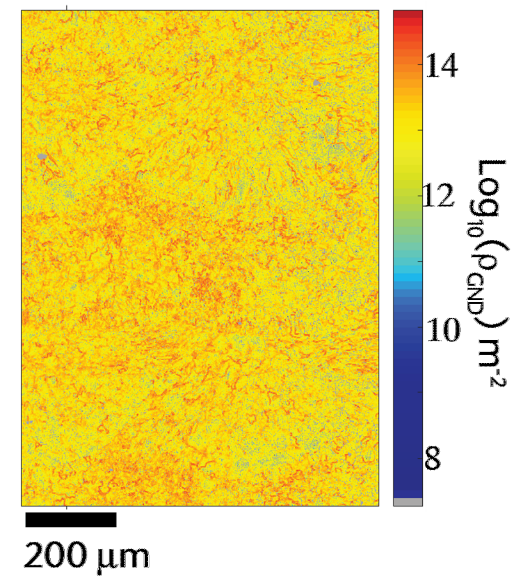

$$\rho_{GND} = \frac{2\theta}{ub} = \frac{2(KAM)}{ub}$$

ρ_{GND} = GND density
b = burgers vector
u = unit length

Calcagnotto, M., et al., Materials Science and Engineering: A, 2010. **527**(10–11): p. 2738-2746.
Lawrence, S.K., et al., Metallurgical and Materials Transactions A, 2014. **45**(10): p. 4307-4315.
Moussa, C., et al., IOP Conference Series: Materials Science and Engineering, 2015. **89**(1): p. 012038.
Kubin, L.P. and A. Mortensen, Scripta Materialia, 2003. **48**(2): p. 119-125.
Gao, H., et al., Journal of the Mechanics and Physics of Solids, 1999. **47**(6): p. 1239-1263.
Kamaya, M., Ultramicroscopy, 2011. **111**(8): p. 1189-1199.

GND Distribution Varies with Build Location

400 W 304L LENS

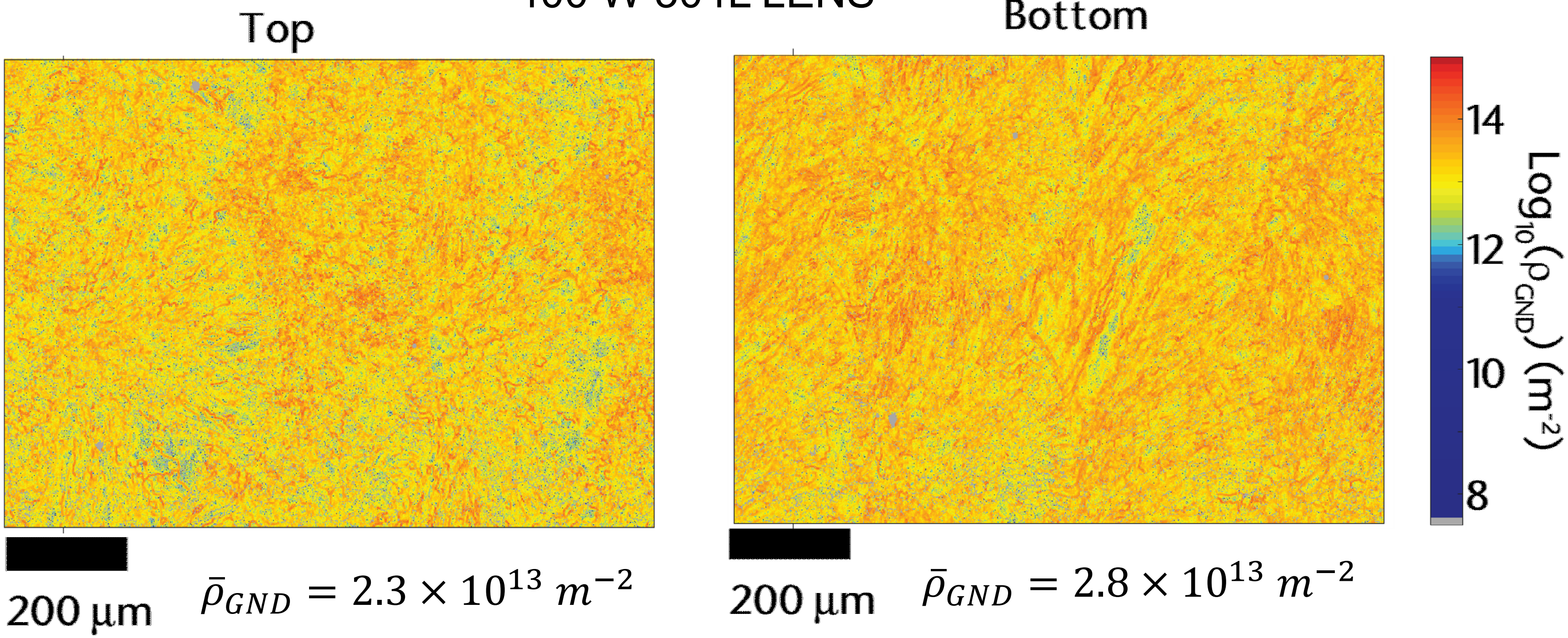

$\bar{\rho}_{GND} = 2.3 \times 10^{13}\ m^{-2}$

$\bar{\rho}_{GND} = 2.8 \times 10^{13}\ m^{-2}$

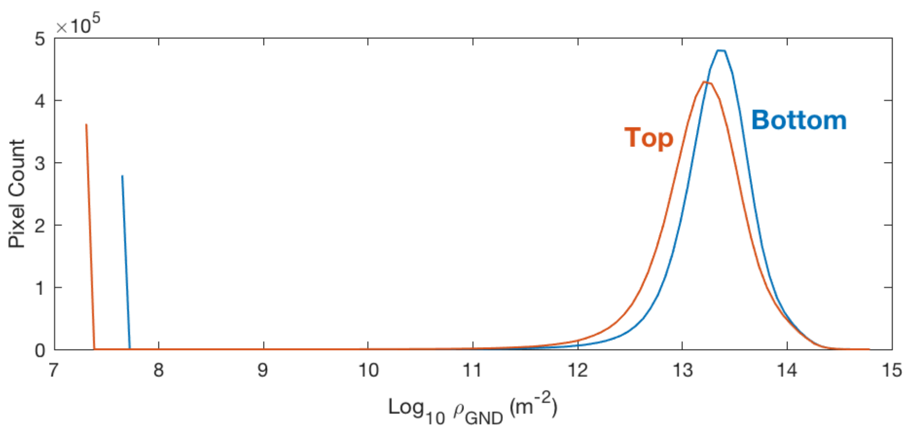

Average GND density and GND distribution show higher densities closer to baseplate

GND Distribution Varies with Build Location

2kW 304L LENS

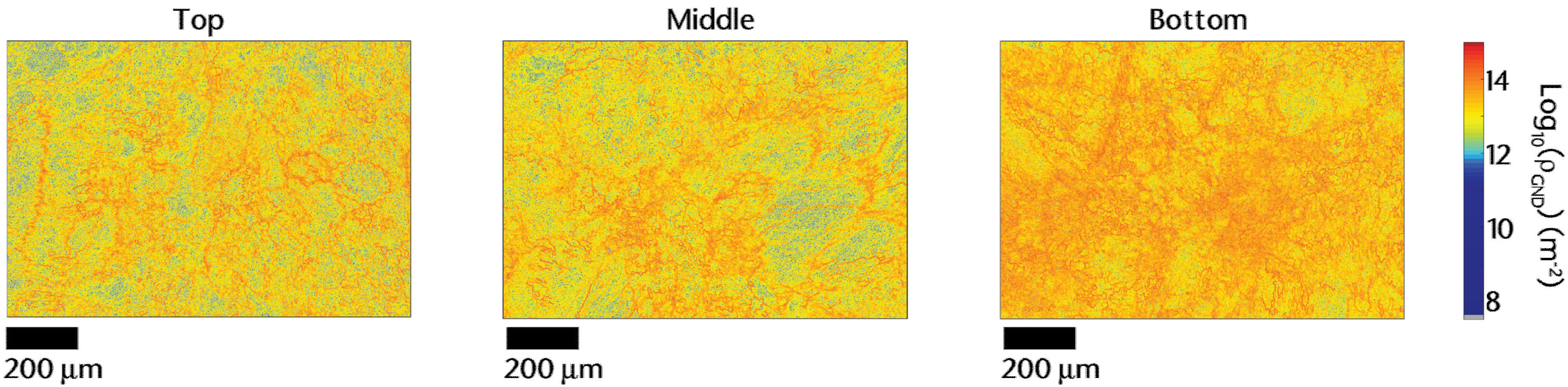

$\bar{\rho}_{GND} = 2.07 \times 10^{13}\ m^{-2}$ $\bar{\rho}_{GND} = 2.09 \times 10^{13}\ m^{-2}$ $\bar{\rho}_{GND} = 3.62 \times 10^{13}\ m^{-2}$

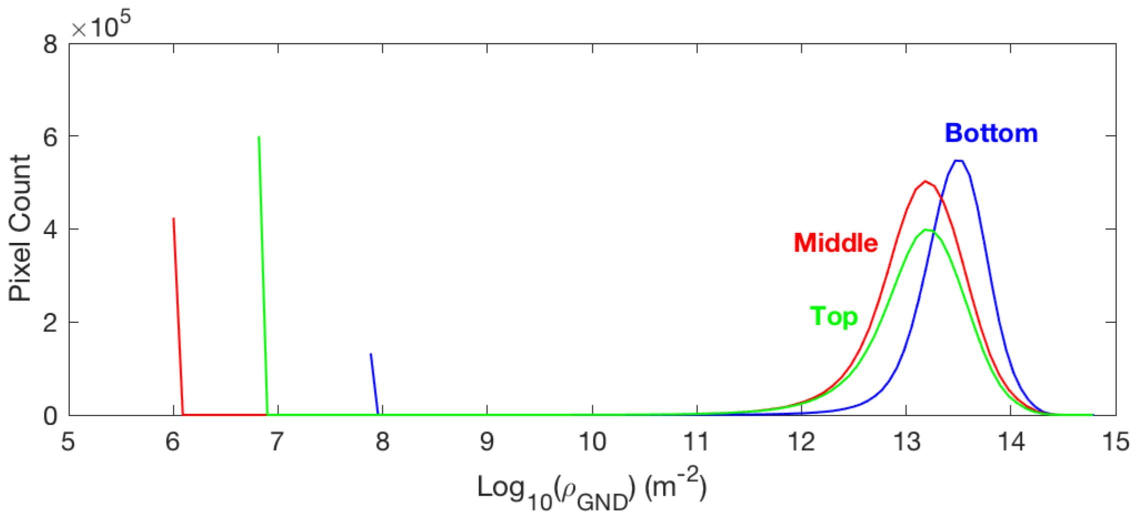

Higher energy builds shows same trend of higher dislocation density closer to the base plate

Plastic Strain Magnitudes Are Highest Near the Baseplate

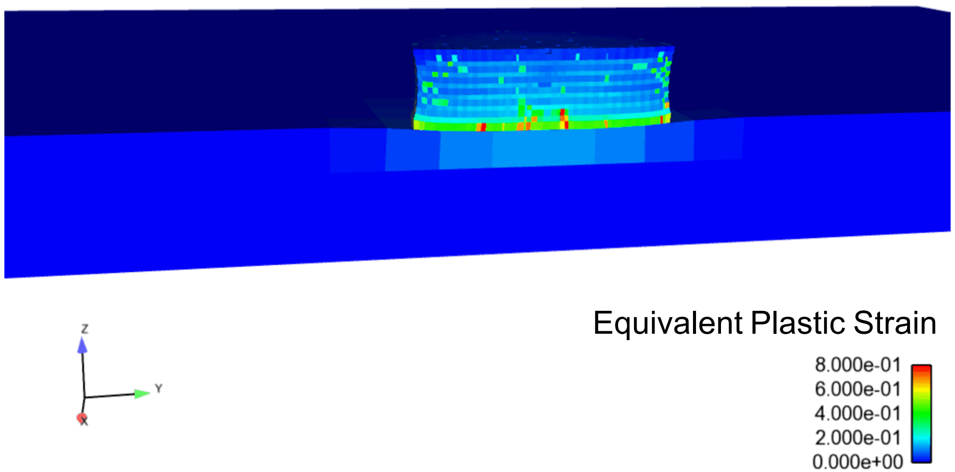

- Explicit model is farther through build showing more depth dependence
  - Different base plate boundary conditions between explicit/implicit

- Implicit model only through second vertical pass shows a similar pattern
  - Note lower overall magnitudes in equivalent plastic strain

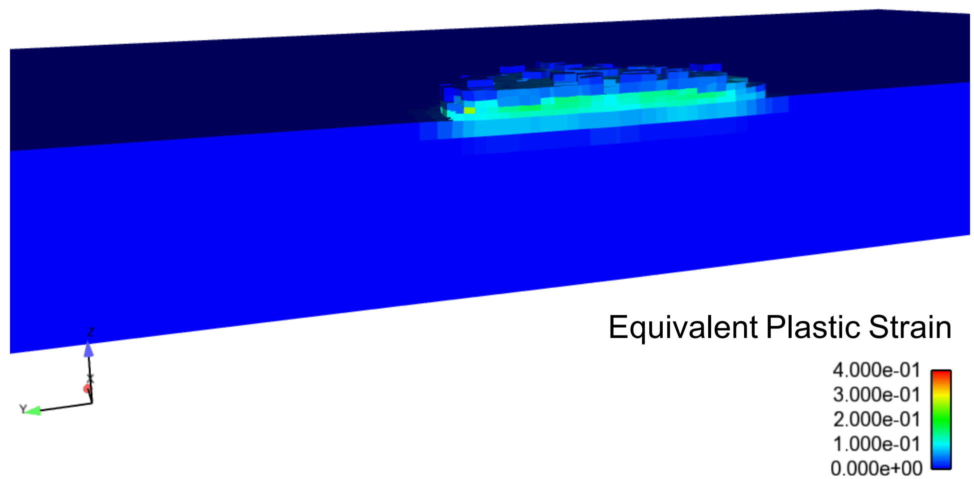

Residual Stress Solutions

Explicit Model

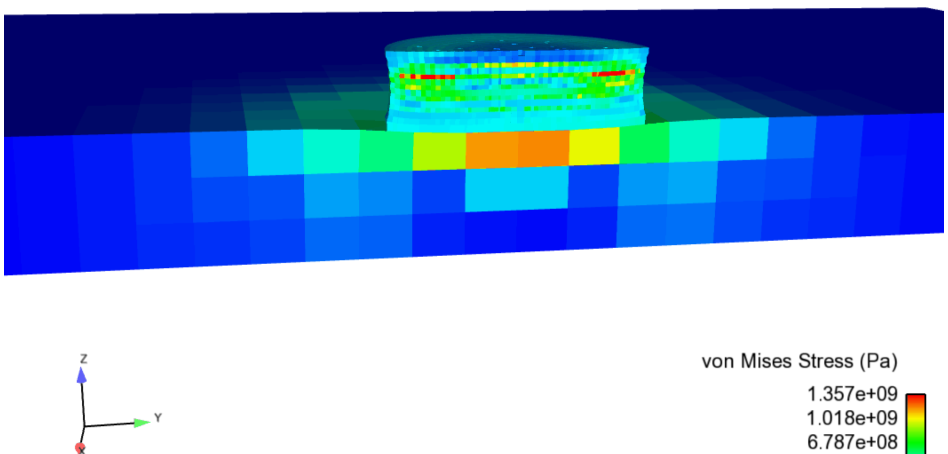

Implicit Model

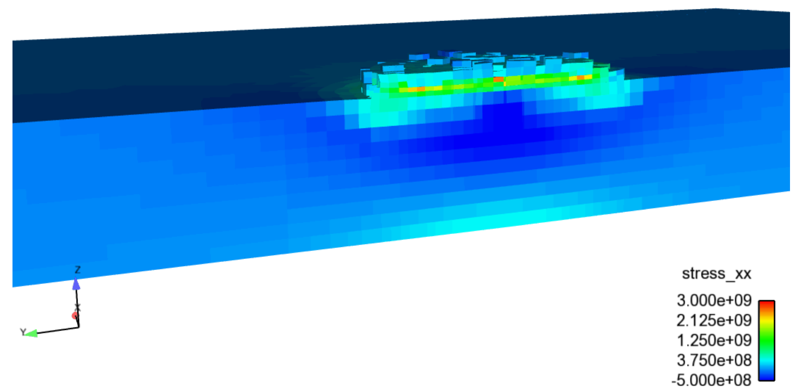

Explicit Model

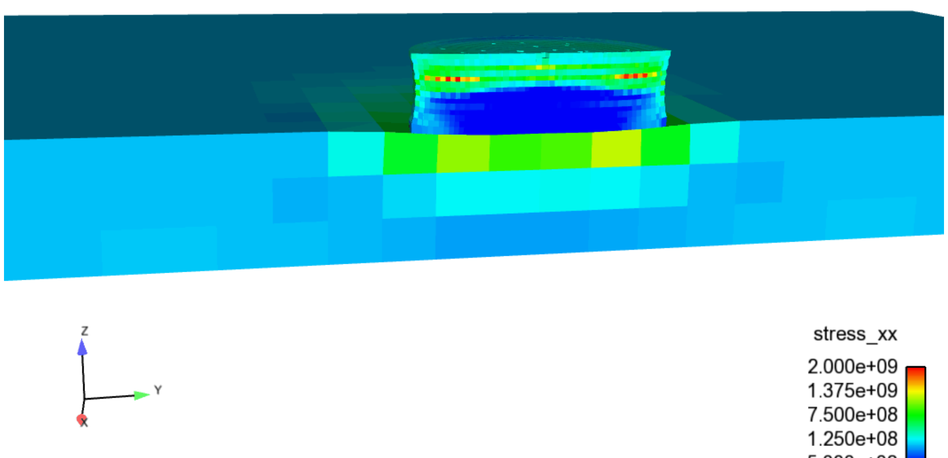

Implicit Model Shows Baseplate Deformations

Initial results show deformation patterns in build plate consistent with previous experimental builds and measurements

- Not present in explicit model because of boundary condition specification on build plate

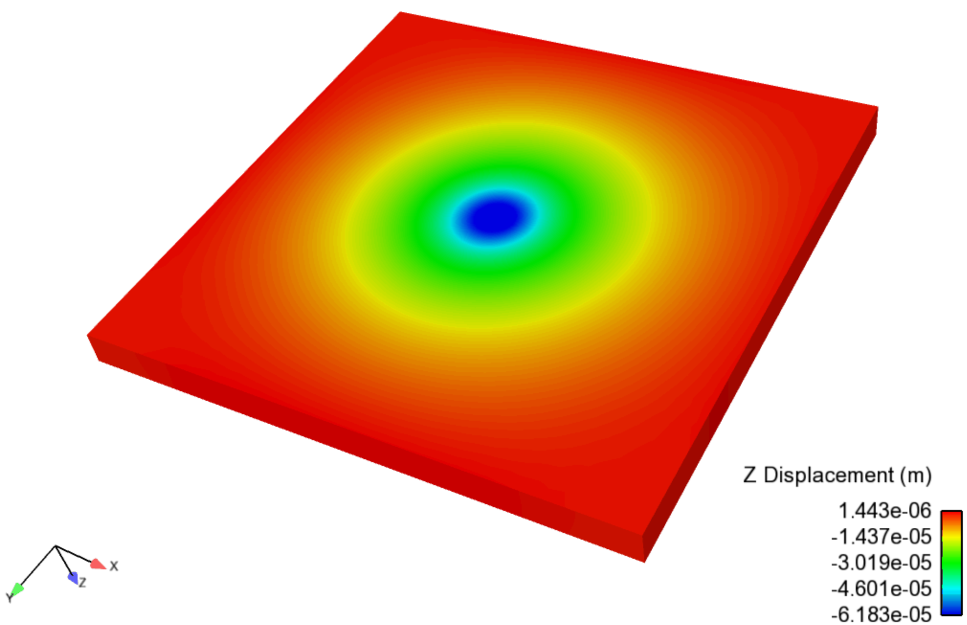

Plate deformation in vertical direction after 2 deposition layers

* Displacements shown 50x

Thermally Induced Plasticity During Processing is Critical

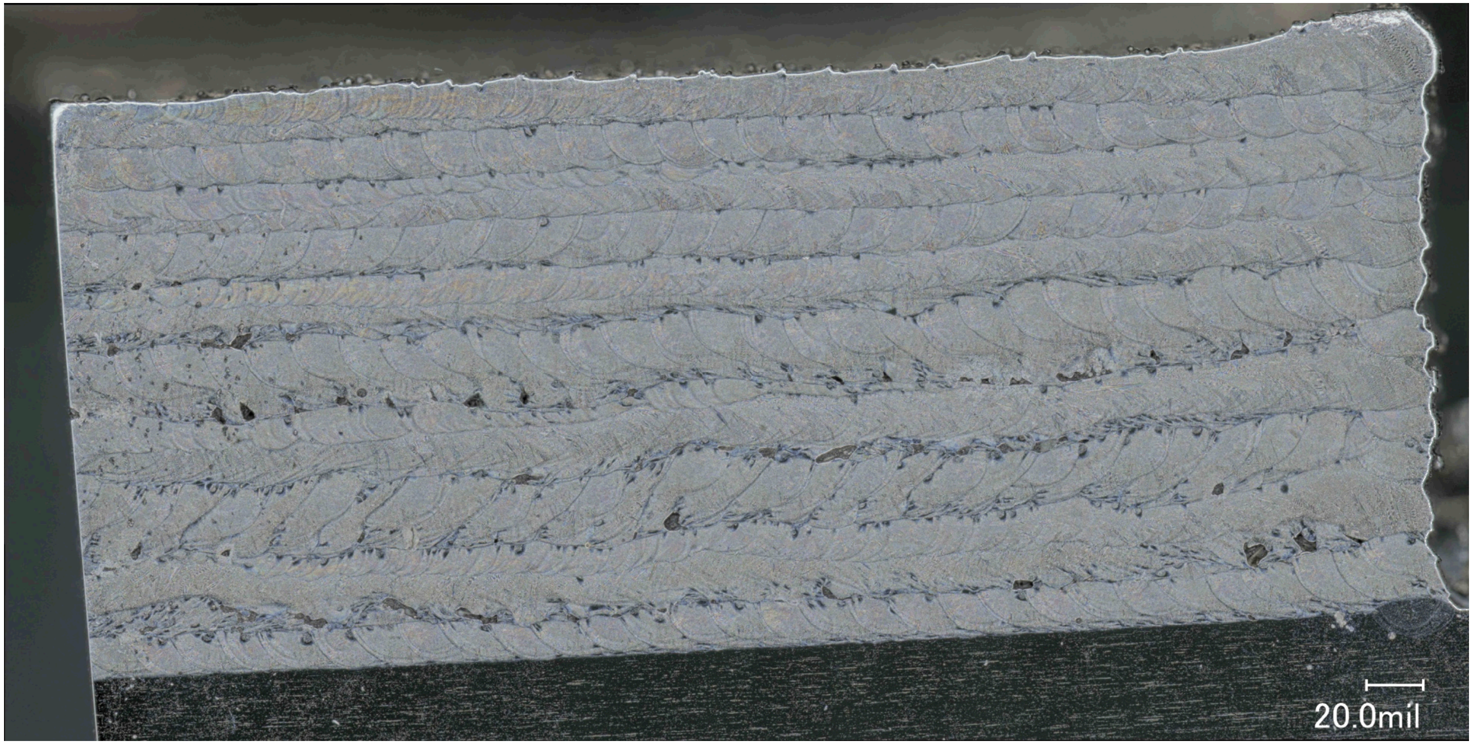

The constraint of the baseplate and thermally induced plasticity during processing make a difference in the dislocation structure and distribution of hardness in LENS 304L stainless steel

This plasticity and the resultant dislocation/hardness/yield distribution are dependent on the geometry of a LENS part

Summary

- Increasing effort is being applied toward part scale builds and improving simulation turnaround time
- Implicit models will be run to completion for button part – *update to follow*
- Coupled thermal-mechanical simulations predict residual stresses values near the material yield strength of 304L stainless steel
- The prediction of yielding and plastic strain near the baseplate is consistent with microstructural measurements of dislocation density
- Experimental verification of residual stresses and simulations of more complex geometries are currently underway

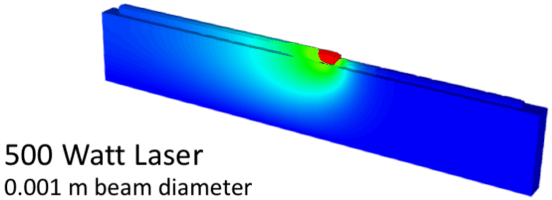

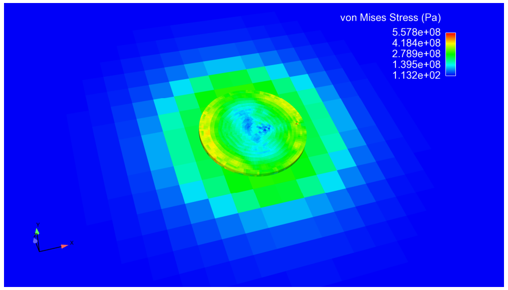

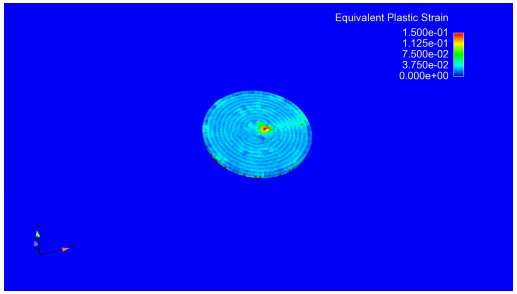

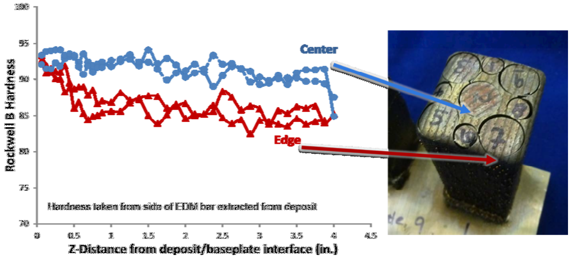

Conclusions

- The thermally-induced strain and resultant dislocation structure is an important factor in understanding the mechanical property variation in a LENS build
  - The effect of the base plate as a heat sink and a mechanical constraint is significant in the development of microstructure
  - We have measured this in simple builds, but the effect could be more problematic in more complicated builds
- Eventually, these models can be used to optimize build parameters for each specific build geometry
  - Laser pattern can be optimized for residual stress before the build (e.g. spiral out, spiral in or cross hatch)

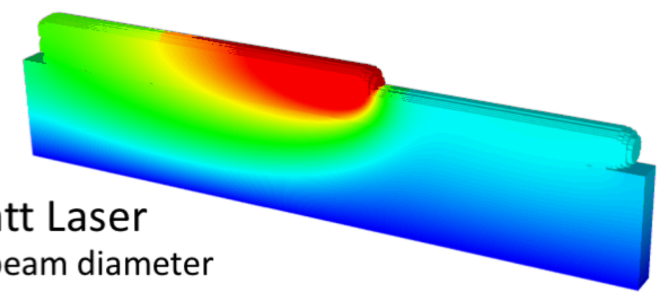

2000 Watt Laser
0.0025 m beam diameter

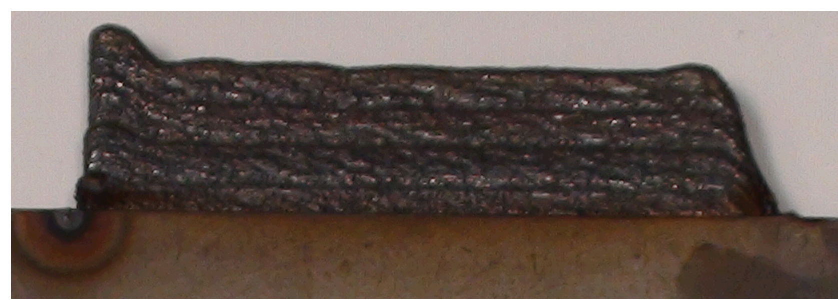

Additional Slides

GND Measurements Correlate With STEM Images of Dislocation Structure

$$\rho_T = \rho_{GND} + \rho_{SSD}$$

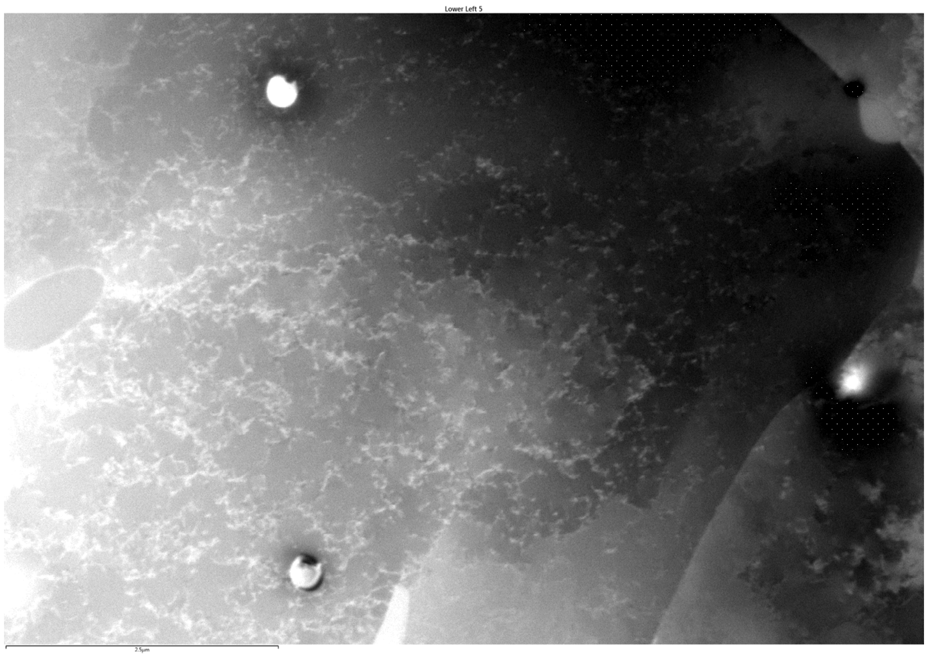

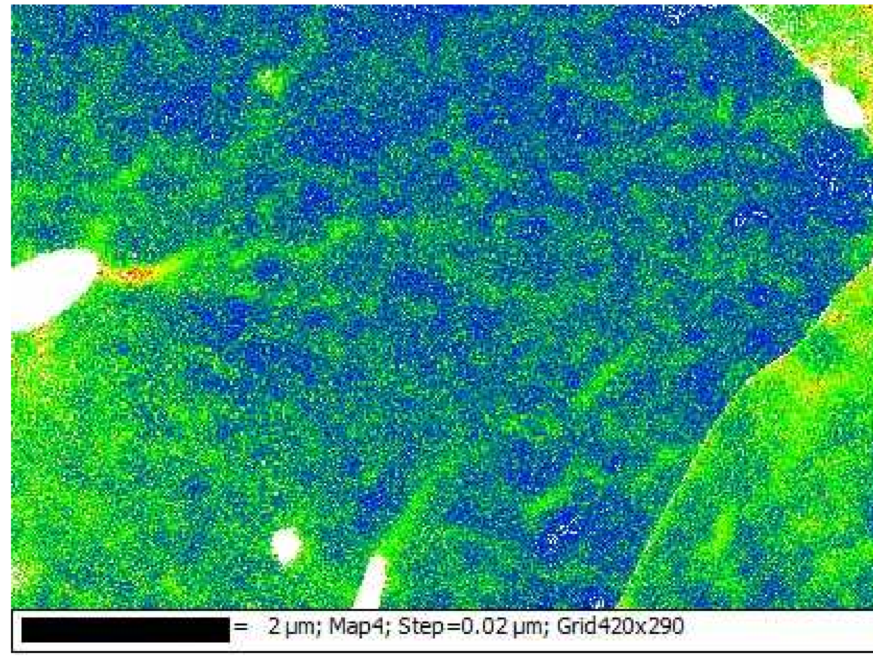

Measurements of local averaged misorientation for GNDs are consistent with images of the more general dislocation structure. Higher misorientations occur where the images show higher dislocations densities.